Controlled modification of erbium lifetime in silicon dioxide with metallic overlayers

Jiming Bao,[a] Nanfang Yu, and Federico Capasso[b]
Harvard School of Engineering and Applied Sciences, Harvard University, Cambridge, Massachusetts 02138, USA

Thomas Mates
Materials Department, University of California, Santa Barbara, California 93106, USA

Mariano Troccoli
Argos Tech, LLC, 3671 Enochs St., Santa Clara, California 95051, USA

Alexey Belyanin[c]
Department of Physics, Texas A&M University, College Station, Texas 77843, USA

(Received 26 March 2007; accepted 27 August 2007; published online 24 September 2007)

The authors report systematic measurements of the lifetime of the 1.54 μm transition of erbium implanted at different energies in SiO_2 films coated with different metals (titanium and chromium). The lifetime shows a strong reduction (up to a factor of 20) with decreasing distance between the erbium and the metal overlay. Their experiments combined with rigorous theoretical modeling demonstrate that a high degree of control over the radiative properties of erbium can be achieved in erbium-implanted materials in a wide range of implantation energies. © *2007 American Institute of Physics*. [DOI: 10.1063/1.2785134]

Erbium is a rare-earth element of paramount technological importance for photonics.[1–3] In bulk SiO_2, the lifetime of Er is determined by its radiative lifetime, due to spontaneous emission, as well as by its nonradiative interactions with the neighboring lattice structure. In lattice relaxed SiO_2 at a low Er concentration, the lifetime of the 1.54 μm transition is of the order of 15 ms and is mainly determined by radiative spontaneous emission.[1,3] It is well known that both the lifetime and the separation between energy levels of atoms are affected by the presence of interfaces with other materials that change the electromagnetic (EM) modes, see, e.g., Refs. 4–8 and references therein. If the interface is located in the *near zone* of an atom, i.e., at a distance much less than the optical transition wavelength, the influence of the interface on the lifetime is mainly due to a semiclassical London–van der Waals interaction rather than to EM vacuum fluctuations. Therefore, it can be adequately described by the change in the total EM reaction field acting on the atom. This approach was shown to provide accurate quantitative results.[9–11] In the case of a finite imaginary part ε_2 of the dielectric constant of the medium adjacent to an atom, the dominant physical mechanism of the lifetime modification is the surface plasmon-mediated energy transfer between the atom and the dissipative medium.[9,12–15] This dissipative energy transfer becomes more effective the smaller the separation between the atom and the medium, thus leading to a shorter lifetime and smaller photoluminescence (PL) intensity.

Recently, Kalkman *et al.* demonstrated enhanced PL decay rate for the Er/silica glass/silver system,[16] but the study was only limited to one Er-implantation depth. In this letter, we present a detailed study of the enhancement of the PL decay rate of the 1.54 μm transition in Er-implanted SiO_2 films coated with different metals and with different Er-implantation energies corresponding to an Er-metal distance much smaller than the transition wavelength ($\lambda/n \approx 1$ μm in SiO_2). Besides the obvious motivation to understand and predict the PL lifetime in these structures, the near-field energy transfer mechanism provides an interesting possibility to control the lifetime of excited electron states in active impurities by varying their distance to the dissipative overlayer and the absorptive properties of the latter.

Samples were prepared by implanting Er^+ on one side of double polished 380-μm-thick silicon wafers with 1 μm of thermally grown SiO_2 on both sides (Implant Sciences Corporation). A dose of 2×10^{13} ions/cm^2 and implantation energies of 10, 20, 40, 80, 150, and 300 keV were used. Samples were annealed in vacuum (1×10^{-7} torr) for 1.5 h at 950 °C to remove implantation related defects. Er ions diffuse minimally under these conditions.[3] The PL spectrum of these samples shows peaks around 1.54 μm, which is a characteristic of the Er $^4I_{13/2}$-$^4I_{15/2}$ transition.[1] Then, an optically thick metal film, typically 160 nm, was thermally deposited on the implanted side of the sample immediately following the annealing step to minimize exposure to water vapor in the air. Without this precaution, the measured lifetimes decrease up to 25% for the shallowest implanted samples over several days. Finally, the samples were annealed in vacuum at 110 °C for 9 h to enhance the quality of the metal films.

The Er concentration profiles were measured by dynamic secondary-ion mass spectrometry (SIMS). These profiles, presented in the inset of Fig. 2, can be fitted with a Gaussian function except for the shallowest implanted samples (10 and 20 keV) that have a comparatively large skewness. The concentration peaks at 13.3, 20.2, 26.6, 42.5, 68.5, and 113.8 nm with full widths at half maximum (FWHMs) of 12.9, 16.0, 17.9, 26.7, 40.2, and 67.6 nm for the above mentioned implantation energies, in agreement with Monte Carlo simulations (SRIM 2003 program).

[a]Electronic mail: jmbao@deas.harvard.edu
[b]Electronic mail: capasso@seas.harvard.edu
[c]Electronic mail: belyanin@physics.tamu.edu

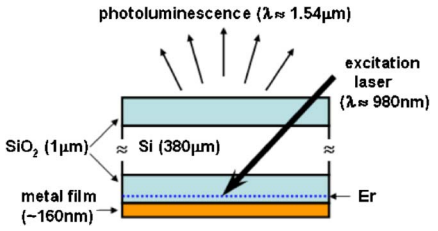

FIG. 1. (Color online) Schematic of the sample structure and excitation configuration.

Time resolved PL measurements were performed at room temperature. A schematic of the experiment is shown in Fig. 1. Square pulses, 50 ms long, from a 980 nm wavelength fiber laser (JDS Uniphase) were collimated and focused onto the nonimplanted side of the samples. The Er PL was collected through a $\lambda=1.4$ μm long wavelength pass filter and focused onto an InGaAs detector (Electro-Optical Systems Inc., long wavelength cutoff at 1.6 μm). Time traces of PL after averaging show smooth decaying tails following the excitation pulses. Typical PL decay curves in logarithmic scale are shown in Fig. 2.

The lifetime of Er embedded in bulk SiO_2 (bulk lifetime) was determined to be $\tau_0=14.3\pm0.3$ ms from the samples with the three largest implantation energies, 80, 150, and 300 keV, since the shallowest implanted samples are more susceptible to water vapor in the air. The bulk lifetime measured is in good agreement with reported values.[3,17] The bulk lifetime was measured in samples prepared by depositing 1 μm SiO_2 onto the Er-implanted side of the annealed samples without metal coating. This ensures that the near field of Er is contained in the SiO_2 and does not interact with any interface.

Measurements were performed for two different metal overlayers, titanium and chromium, with complex refractive indices $3.68+4.61i$ and $3.67+4.19i$ at $\lambda=1.54$ μm, respectively.[18] Measured decay rates of the metal coated samples for six implantation depths are indicated by blue circles in Fig. 3. They are obtained by fitting with an exponential curve the initial part of the PL signal, during which the signal drops by approximately a factor of 5 from its maximum value. For the 10 and 20 keV implants, the measured decay rates were corrected for the detector response time (~0.2 ms). It was found that the decay is generally nonexponential: it slows down with time, which is due to the spreading of ions along the direction of implantation. The variation in the lifetimes measured laterally from different spots across the wafer is ±5%. The PL intensity decreases with decreasing implantation depth. Furthermore, PL intensities are higher for samples without metallic coating. The above is consistent with the nature of the Er-metal interaction, as discussed earlier in the letter.

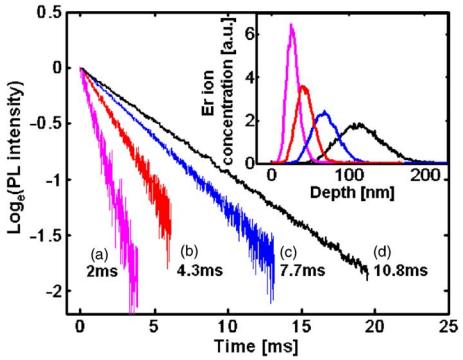

FIG. 2. (Color online) Erbium photoluminescence intensity decay curves for a variety of implantation energies and metal coatings: (a) Ti coated, 40 keV Er; (b) Cr coated, 80 keV Er; (c) Ti coated, 150 keV Er; and (d) Cr coated, 300 keV Er. Shown are the corresponding lifetimes. Intensities are normalized to their corresponding maxima before taking logarithm. Inset (from left to right): measured SIMS profiles of the Er ions implanted at the energies of 40, 80, 150, and 300 keV as a function of distance from the metal/SiO_2 interface.

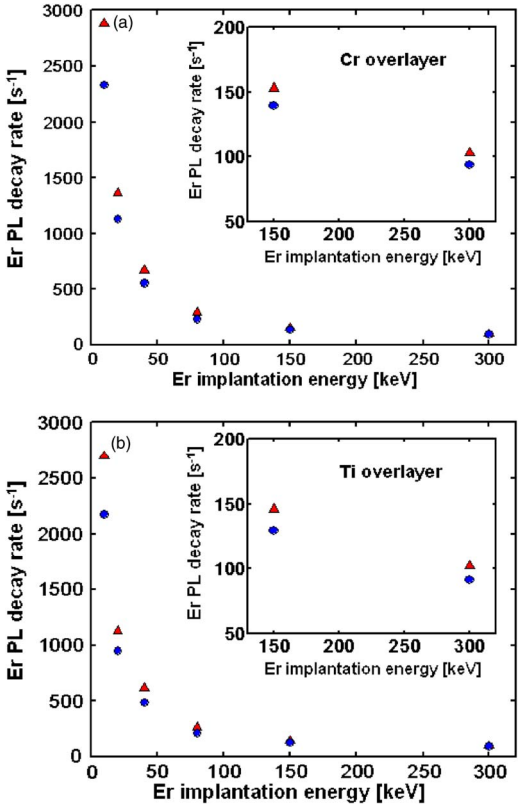

FIG. 3. (Color online) Experimental (blue circle) and theoretical (red triangle) Er photoluminescence decay rates for samples with (a) Cr and (b) Ti overlayers. Inset: zoom-in view of the two points with the highest implantation energies. For the Cr coated samples and an increasing implantation energy, the relative errors of the theoretical decay rates are ±10%, ±10%, ±5%, ±4%, ±2%, and ±1%; the relative errors of the experimental decay rates are ±10%, ±7%, ±5%, ±5%, ±5%, and ±3%. Similarly, for the Ti coated samples and an increasing implantation energy, the relative errors of the theoretical decay rates are ±10%, ±10%, ±5%, ±4%, ±2%, and ±1%; the relative errors of the experimental decay rates are ±12%, ±8%, ±6%, ±5%, ±5%, and ±3%. The errors of the theoretical data are mainly due to an uncertainty in determining the Er-implantation depth. The latter was used for theoretical calculations. The errors in the experimental data are mainly due to the variation in the lifetimes measured in different spots across the wafer.

Theoretically, the measured bulk decay rate $\Gamma_0=1/\tau_0 \approx 70\ s^{-1}$ can be separated into the radiative and the bulk nonradiative contributions, $\Gamma_0=\Gamma_0^{rad}+\Gamma_0^{nr}$. The presence of the metal overlayer will change the radiative decay rate Γ_0^{rad}, but it will largely leave the bulk nonradiative decay rate Γ_0^{nr} unaffected because it is due to the neighboring atoms of the implanted ions. For a given implantation energy E, the total decay rate with metal coating can then be written as

$$\Gamma^{tot}(E)=\Gamma(E)+\Gamma_0^{nr}. \quad (1)$$

Our PL decay experiments measure $\Gamma^{tot}(E)$ (blue circles in Fig. 3). The modified radiative decay rate $\Gamma(E)$ can be

calculated in two steps. First, we consider the expression for the decay rate of a single atom in the vicinity of a dissipative medium.[14,15] For a dipole with transverse and parallel orientations with respect to the interface, the decay rates are[14,15]

$$\gamma_t = \Gamma_0^{\mathrm{rad}}\left\{1 - \tfrac{3}{2}\,\mathrm{Im}\left(\int_0^\infty R_p \frac{u^3}{a_1}\exp(-4\pi n_1 a_1 z/\lambda)du\right)\right\}, \tag{2}$$

$$\gamma_p = \Gamma_0^{\mathrm{rad}}\left\{1 + \tfrac{3}{4}\,\mathrm{Im}\left(\int_0^\infty [(1-u^2)R_p + R_t]\frac{u}{a_1}\exp(-4\pi n_1 a_1 z/\lambda)du\right)\right\}, \tag{3}$$

where z is the distance of a dipole from the dissipative medium (e.g., metal),

$$R_t = \frac{a_1 - a_2}{a_1 + a_2}, \quad R_p = \frac{\varepsilon_1 a_2 - \varepsilon_2 a_1}{\varepsilon_1 a_2 + \varepsilon_2 a_1},$$

$$a_1 = -i\sqrt{1-u^2}, \quad a_2 = -i\sqrt{\varepsilon_2/\varepsilon_1 - u^2}.$$

ε_1 is the dielectric constant of SiO_2 and ε_2 is the dielectric constant of the overlayer. Formulas (2) and (3) are in exact agreement with Eqs. (2.17) and (2.29) obtained in Ref. 9 on the basis of Hertz vectors formalism. They include relevant effects such as reflection of the EM field, excitation of the surface plasmons, and dissipation in the overlayer. Then, using the distribution $f(z)$ of implanted Er ions measured in the SIMS experiment, the time dependence of the intensity can be calculated as $I(t) \propto \int f(z)\exp(-\gamma(z)t)dz$, where $\gamma(z)$ is the decay rate for an atom at a distance z from the interface, averaged over random dipole orientation, $\gamma(z) = (\gamma_t + 2\gamma_p)/3$. The resulting time dependence $I(t)$ is slightly nonexponential. The normalized radiative decay rate $\Gamma(E)/\Gamma_0^{\mathrm{rad}}$ is obtained by fitting with an exponential dependence only the initial part of the computed function $I(t)$, in correspondence with the experimental procedure. $\Gamma(E)$ is plotted with red triangles in Fig. 3, assuming that the radiative efficiency of erbium in bulk SiO_2 is 100%, $q \equiv \Gamma_0^{\mathrm{rad}}/\Gamma_0 = 1$, or $\Gamma_0^{\mathrm{rad}} = \Gamma_0$ in Eqs. (2) and (3). As is clear from Fig. 3, the theoretical points are uniformly shifted up from the experimental points, which indicate that the radiative efficiency is, in fact, smaller than unity. By attributing the difference between theoretical and experimental points to the nonradiative decay, the radiative efficiency can be obtained for each implantation energy from the measured total decay rate $\Gamma^{\mathrm{tot}}(E)$ and the calculated normalized radiative decay rate $\Gamma(E)/\Gamma_0^{\mathrm{rad}}$ as[13]

$$q = \frac{\Gamma_0^{\mathrm{rad}}}{\Gamma_0} = \frac{(\Gamma^{\mathrm{tot}}(E)/\Gamma_0) - 1}{(\Gamma(E)/\Gamma_0^{\mathrm{rad}}) - 1}. \tag{4}$$

If the nonradiative decay does not depend on E, we should obtain the same value of q for all implantation energies. In reality, there is some sample-to-sample variation: for Cr samples at six implantation energies 10, 20, 40, 80, 150, and 300 keV, we obtain efficiencies equal to 0.65, 0.81, 0.81, 0.74, 0.83, and 0.72, respectively. For Ti coated samples, we obtain efficiencies equal to 0.62, 0.73, 0.76, 0.72, 0.78, and 0.68, respectively. The q deduced for the larger implantation energies is in the range of reported values.[1,3,11,19]

Error bars for the theoretical points in Fig. 3 are calculated by shifting the SIMS profiles by ±1.5 nm, which is the estimated error of the SIMS measurements. The error is mainly due to an uncertainty in determining the position of SiO_2 surface in the SIMS experiment.

Our results indicate that the decay rate of the 1.54 μm optical transition in Er-implanted samples can be strongly enhanced in a well-controllable and predictable way by changing the separation between Er ions and the metal coating. This creates the obvious possibility of enhancing the modulation rate and controlling saturation nonlinearity in devices implanted or doped with Er or other active impurities. Furthermore, our measurements allow an estimation of the radiative efficiency of the 1.54 μm transition in implanted Er, which is a crucial parameter for optical devices.

This work is sponsored by the Nanoscale Science and Engineering Center (NSEC) at Harvard University and the Air Force Office of Scientific Research (AFOSR MURI on Plasmonics). One of the authors (A.B.) acknowledges the support by NSF CAREER Grant No. ECS-0547019. Another author (T.M.) acknowledges support from the NSF under Grant No. DMR05-20415 for the use of UCSB analytical facilities. It is a pleasure to thank Frans Spaepen, Michael Aziz, Harry Atwater, Cheng-Yen Wen, Dawen Pang, Joseph Chen, Mengyan Shen, Laurent Diehl, and Marko Loncar for suggestions and collaborations. Support from the Center for Nanoscale Systems (CNS) at Harvard University is also gratefully acknowledged. Harvard-CNS is a member of the National Nanotechnology Infrastructure Network (NNIN).

[1] E. Desurvire, *Erbium-Doped Fiber Amplifiers, Principles and Applications* (Wiley-Interscience, New York, 2002), Chap. 4, p. 233; Chap. 6, p. 455.
[2] A. Polman, B. Min, J. Kalkman, T. J. Kippenberg, and K. J. Vahala, Appl. Phys. Lett. **84**, 1037 (2004).
[3] A. Polman, J. Appl. Phys. **82**, 1 (1997).
[4] E. A. Hinds, *Advances in Atomic, Molecular and Optical Physics* (Academic, Boston, 1991), Vol. 28, p. 237.
[5] D. Meschede, Phys. Rep. **211**, 201 (1992).
[6] I. Suemune, A. Ueta, A. Avramescu, S. Tanaka, H. Kumano, and K. Uesugi, Appl. Phys. Lett. **74**, 1963 (1999).
[7] T. Quang, M. Woldeyohannes, S. John, and G. S. Agarwal, Phys. Rev. Lett. **79**, 5238 (1997).
[8] K. J. Vahala, Nature (London) **424**, 839 (2006).
[9] R. R. Chance, A. Prock, and R. Silbey, *Advances in Chemical Physics* (Wiley, New York, 1978), Vol. XXXVII, p. 1.
[10] K. H. Drexhage, H. Kuhn, and F. P. Schafer, Ber. Bunsenges. Phys. Chem. **72**, 329 (1968); R. R. Chance, A. Prock, and R. Silbey, J. Chem. Phys. **60**, 2184 (1974).
[11] E. Snoeks, A. Lagendijk, and A. Polman, Phys. Rev. Lett. **74**, 2459 (1995).
[12] A. A. Belyanin, V. V. Kocharovsky, Vl. V. Kocharovsky, and F. Capasso, Phys. Rev. Lett. **88**, 053602 (2002).
[13] X. Brokmann, L. Coolen, M. Dahan, and J. P. Hermier, Phys. Rev. Lett. **93**, 107403 (2004).
[14] V. V. Kocharovsky, Vl. V. Kocharovsky, and A. A. Belyanin, Phys. Rev. Lett. **76**, 3285 (1996).
[15] A. A. Belyanin, V. V. Kocharovsky, and VI. V. Kocharovsky, Laser Phys. **5**, 1164 (1996).
[16] J. Kalkman, L. Kuipers, A. Polman, and H. Gersen, Appl. Phys. Lett. **86**, 041113 (2005).
[17] A. M. Vredenberg, N. E. J. Hunt, E. F. Schubert, D. C. Jacobson, J. M. Poate, and G. J. Zydzik, Phys. Rev. Lett. **71**, 517 (1993).
[18] P. B. Johnson and R. W. Christy, Phys. Rev. B **9**, 5056 (1974).
[19] M. J. A. de Dood, L. H. Slooff, A. Polman, A. Moroz, and A. van Blaaderen, Phys. Rev. A **64**, 033807 (2001).